Pergamon

International Journal of Machine Tools & Manufacture 39 (1999) 651–667

INTERNATIONAL JOURNAL OF
MACHINE TOOLS
& MANUFACTURE
DESIGN, RESEARCH AND APPLICATION

Fundamental geometry analysis of wire electrical discharge machining in corner cutting

W.J. Hsue, Y.S. Liao*, S.S. Lu

Department of Mechanical Engineering, National Taiwan University, No. 1 Roosevelt Rd. Sec. 4, Taipei, Taiwan, ROC

Received 9 October 1997

Abstract

Fundamental geometry properties of wire electrical discharge machining (WEDM) process in corner cutting is studied. The concept of discharge-angle is introduced, and its mathematical expression is derived by analytical geometry. A model to estimate the metal removal rate (MRR) in geometrical cutting is developed by considering wire deflection with transformed exponential trajectory of wire centre. The computed MRR is compared with measured sparking frequency of the process since they are equivalent to each other for an iso-energy type machine. A very good agreement is obtained. Both of the discharge-angle and MRR drop drastically to a minimum value depending on the corner angle being cut as the guides arrive at the corner apex, and then recover to the same level of straight-path cutting sluggishly. Hence the observed phenomenon of increased gap-voltage and decreased sparking frequency in corner cutting can be physically interpreted. In addition, the variation of the machining load caused by the change of MRR, which was taken as unknown disturbance in the past, can be predicted and used for control purpose.

Nomenclature

C_θ	discharge-angle of WEDM process
R	discharge-radius of WEDM process
θ	angle of a corner path
dL	small displacement of wire electrode

* Corresponding author. Tel.: + 886-2-23626431; Fax: + 886-2-23631755; E-mail: liaoys@cc.ntu.edu.tw

0890-6955/99/$—see front matter
PII: S0890-6955(98)00046-7

O	apex of an angular corner
P	intersection point of discharge-circle and the boundary of kerf
ϕ	upper intersection angle of the discharge-angle
θ	lower intersection angle of the discharge-angle
h, $h(k)$	uncut thickness of workpiece and its form in discrete time system
dA	a small cut area of WEDM process
u	machine feedrate of WEDM process
ΔT	sampling period
V_r	theoretical metal removal volume
H	workpiece height
δ	wire lag behind guides in the straight-path cutting
b	curve fitting parameter of wire trajectory
$\mathbf{M}_\theta$	transformation matrix for wire trajectory
$\vec{g}$	dragging force of guides
$\vec{e}$	resultant discharging load exerted on wire
$\vec{n}$	resultant of guide's dragging force and discharging load
θ_T	tangent angle at an arbitrary point of the wire trajectory
n	slope of guide's path in the x–y coordinate system
m	slope of guide's dragging force in the x–y coordinate system
θ_G	directional angle of guide's dragging at an arbitrary point of wire trajectory
x_G	x coordinate of guide's position in the x–y coordinate system
α	directional angle of the resultant load exerted on the wire
f_T	sparking frequency of WEDM process
f_r	sparking frequency distributed along a unit length of workpiece
P	normal load exerted on the wire electrode
Q	lateral load exerted on the wire electrode
β	angle of a small sector relative to tangent of the wire trajectory
$d\beta$	a small angle occupied by a small sector

1. Introduction

Being a highly precise process and independent of material hardness, Wire Electrical Discharge Machining (WEDM) is a very promising machining operation to meet diverse requirements in the rapidly growing production field. Moreover, it is such an important operation that, in some manufacturing areas, WEDM is the only choice in the right time and at a justified cost [1]. There have been many researches on WEDM in the past, most of them focused on straight-path cutting [2–9]. While various methods on the improvement of geometrical accuracy have been studied [10–12], the fundamental mechanism of geometrical inaccuracy in corner cutting has not been investigated and understood comprehensively.

In an early paper of fundamental study on geometrical cutting, Dekeyser et al. [1] showed that the main causes of geometrical inaccuracy might be attributed to the preferential occurrence of

discharge at the corner edge and the enhanced vibration resulted from asymmetric load exerted on the wire. However, the quantitative analysis about the mechanism of preferential discharge and enhanced wire vibration was still absent. Moreover, in most application of practical WEDM, the gap-voltage is adapted as a feedback for the servo-feed controller. The sudden increase of gap-voltage in corner cutting, which caused not only the risk of wire rupture, but also the geometrical inaccuracy was not discussed very clearly.

Furthermore, most of the previous studies on geometrical cutting were concentrated on the wire deflection phenomenon [10–12]. Some of them proposed path compensation strategies to correct the inaccuracy of geometrical cutting in an off-line [1,12] or on-line manner [11]. But the barrel-shape inaccuracy of workpiece still existed, since wire deflection was not improved significantly in the proposed strategies. Recently, Magara et al. [13] showed that wire deflection can be significantly reduced by changing machining conditions such as feedrate and off-time. By so doing, both geometrical accuracy and straightness along workpiece height were improved. However, their strategy was quite intuitive and there were no analytical bases for the tuning of machining conditions. In their second report on the finish-cutting process [14], the metal removal, which was defined as the ratio of the removal area with respect to speed of wire centre, was calculated. However, the general mechanism of metal removal in rough cutting was still not exposed.

The purposes of this paper are to study the fundamental geometry properties of WEDM, and to interpret the phenomenon of increased gap-voltage and the decreased sparking frequency around corners in general rough cutting. By computing the variation of metal removal rate (MRR), it is expected to provide an analytical base and an accurate prediction for the control strategies of tuning machining conditions.

In this paper, the concept of discharge-angle of WEDM is introduced. Assuming that the actual cutting kerf around a corner is given, the mathematical expression of discharge-angle is derived by analytical geometry. By using the discharge-angle, the variation of MRR in corner cutting is computed with a simple formula. The computed MRR is compared with the measured sparking frequency, since they are equivalent for an iso-energy type machine. Some phenomena appeared in corner cutting are interpreted.

Generally speaking, the fundamental geometrical cutting may be categorized into angular corner and circular arc. An arc may be taken as the composition of a series of straight line segment. Therefore, only the geometry analysis in machining angular corners is considered in this paper.

2. Geometrical analysis

2.1. Definition and properties of discharge-angle and MRR

Fig. 1(a) shows the geometrical configuration of WEDM process. As illustrated by the dashed line, the deflected wire inside the workpiece can be considered as a rigid rod due to its averaged effect.

Taking a top view of workpiece and wire electrode in WEDM as shown in Fig. 1(b), the discharge-angle, C_θ, of this cutting process is defined as the possible angular range spanned by electrical arcs between both electrodes in a small period of time. Possible sparks can be emitted from any point around the wire surface. However, the actual discharging sparks would be most

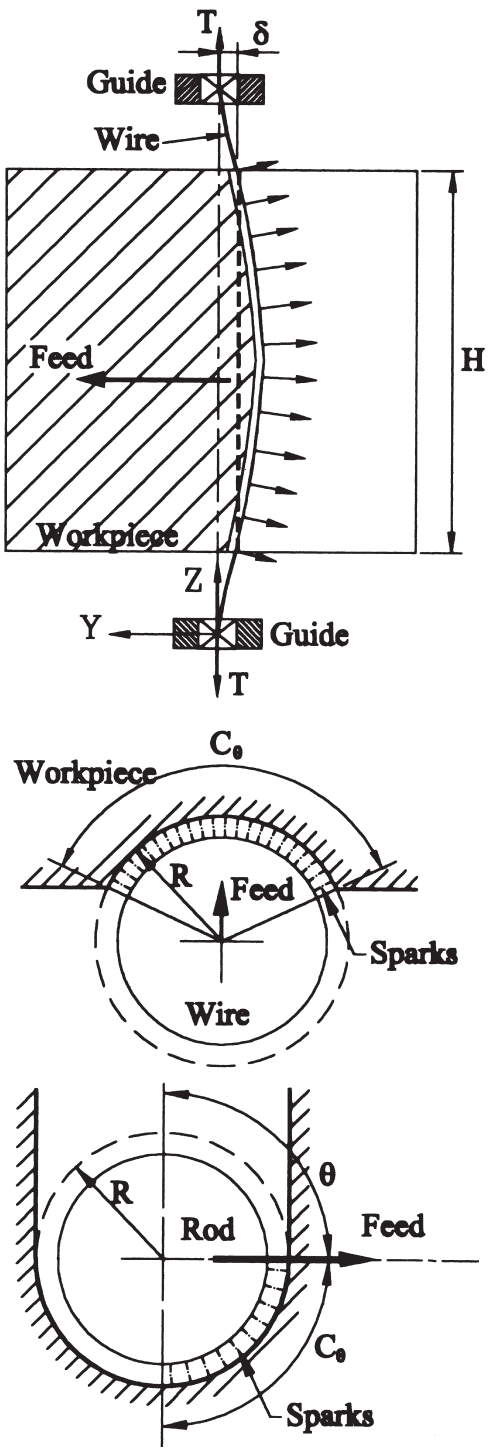

Fig. 1. (a) Configuration of WEDM process; (b) definition of discharge-angle C_θ.

likely distributed along a circular arc in front of the wire in the feed direction, since electricity field established between both electrodes always breaks down at the nearest distance.

The possible discharge-angle in general straight-path cutting is equal to π, and it is smaller than π at the beginning of cutting around an edge of the workpiece, as shown in the upper part of Fig. 1(b). Moreover, if a rigid rod passing through the guides is used instead of the wire, then the discharge-angle at the instant of turning a corner is equal to the corners angle. For example, as shown in the lower part of Fig. 1(b), C_θ is equal to $\pi/2$ as the rod is turning a right-angle.

Referring to the upper part of Fig. 1(b), the discharge-radius, R, is defined as the radius of the front end of electrical sparks. The cutting process may virtually be imagined as the progression of a moving discharge-circle which is represented with a dashed line circle. The discharge-circle with the same centre of the wire electrode has certain discharge-radius depending on the machining conditions (such as power conditions and machine feedrate).

The variation of MRR is important to the fundamental studies of corner cutting process, such as the discharging load imposing on the wire and the causes of geometrical inaccuracy. A computational model of MRR is schematically shown in Fig. 2 assuming that the discharge-angle is known.

Considering that the discharge-angle varies from C_θ to C_θ' as the wire centre moves from W_1 to W_2 at time instants t_1 and t_2, respectively. For simplification, the discharge-radius is assumed to be constant. Suppose the workpiece to be cut by WEDM has a uniform height, H, the removal volume between instants t_1 and t_2 can be obtained as follows:

$$V_r = \int_{t1}^{t2} u(t)\cdot H\cdot R\cdot[1 - \cos C_\theta(t)]\mathrm{d}t \tag{1}$$

where $u(t)$ and $C_\theta(t)$ represent feedrate of the machine and discharge-angle at any instant t, respectively.

Thus, the MRR can be derived by the derivative of V_r with respect to time t, or

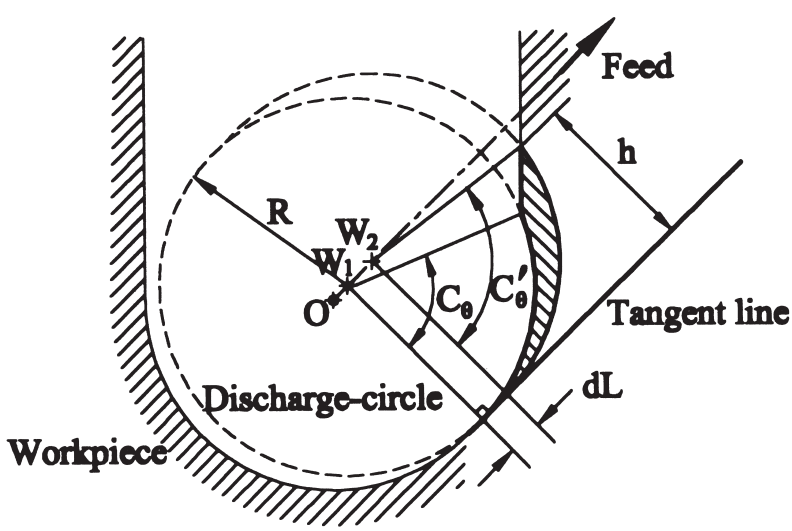

Fig. 2. Metal removal area swept by the varying discharge angle.

$$\mathrm{MRR} = \frac{dV_r}{dt} \tag{2}$$

For practical computation in the discrete time system with sampling interval ΔT, it is convenient to approximate the removal rate by the trapezoidal rule. Let $h(k) = R[1 - \cos C_\theta(k)]$ represent the uncut thickness of workpiece at the kth sampling instant, then, the theoretical MRR in machining a small displacement dL can be rewritten as:

$$\mathrm{MRR} \cong H \cdot dL \cdot \frac{h(k) + h(k+1)}{2\,\Delta T} \tag{3}$$

For example, the discharge-angle is π in straight-path cutting, and the thickness to be cut is $h(k) = R[1 - \cos\pi] = 2R$. Hence, from Eq. (3), the metal removal rate in straight path cutting is $2R\,HdL/\Delta T$.

2.2. Computational model of MRR in corner cutting

The MRR in corner cutting is quite different from that in straight-path cutting. Because the actual wire position is unknown, it is difficult to obtain the MRR in the actual corner cutting. However, by certain simplification, the systematic analysis of metal removal rate can be obtained with the proposed concept of discharge-angle. For simplification, the following basic assumptions are required:

1. The kerf (cut groove) of WEDM corner cutting is known.
2. The power source of WEDM is of iso-energy type, and the discharge-radius is assumed to be constant.
3. The feedrate of machine around a corner is slow.

Considering the actual kerf (cut groove) of a right-angle cutting as shown in Fig. 3(a), the trajectory of the wire centre in corner cutting can be obtained from the narrowed kerf, as illustrated by the centre-line in the figure. Let the wire lag behind guides at corner apex be denoted by δ, then the actual trajectory of wire centre can be fitted to an exponential function of the following form.

$$y = \delta \exp(-x/b) \tag{4}$$

where b is a parameter relating to machining conditions. The positive variable, x, represents the displacement of guides relative to apex of the corner on the workpiece.

In order to simplify the derivation of C_θ and MRR in practical corner cutting, the exponential function given by Eq. (4) is transformed to describe the trajectory of wire centre in cutting corners other than $\pi/2$. The coordinate transformation can be carried out by the following equation:

$$\begin{pmatrix} \bar{x} \\ \bar{y} \end{pmatrix} = \mathbf{M}_\theta \begin{pmatrix} x \\ y \end{pmatrix} \tag{5}$$

where $\mathbf{M}_\theta$ is the transformation matrix depending on the corner angle θ. For an acute corner, i.e. $\theta < \pi/2$, $\mathbf{M}_\theta$ is

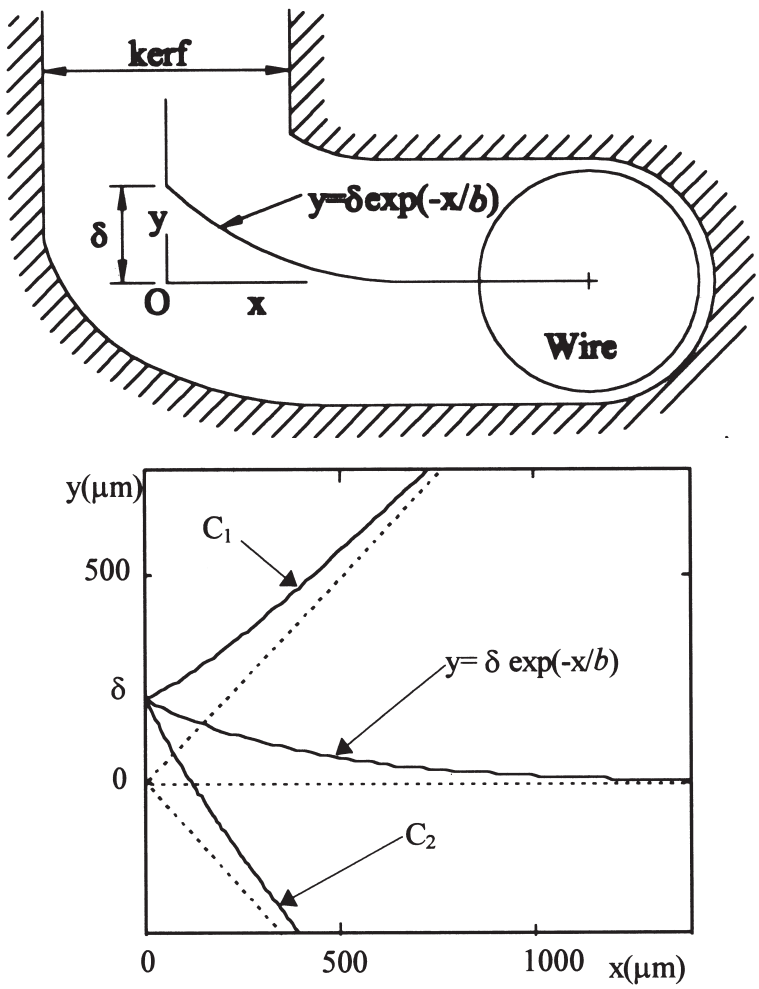

Fig. 3. (a) Kerf (cut groove) of a right-angle cutting and the fitted wire trajectory. (b) Fitted wire trajectory of a right-angle corner, $\pi/4$ corner (curve C_1) and $3\pi/4$ corner (curve C_2).

$$\mathbf{M}_\theta = \begin{bmatrix} 1 & 0 \\ \tan(\frac{\pi}{2} - \theta) & 1 \end{bmatrix} = \mathbf{M}_1 \tag{6}$$

Otherwise,

$$\mathbf{M}_\theta = \begin{bmatrix} \cos(\frac{\pi}{2} - \theta) & 0 \\ \sin(\frac{\pi}{2} - \theta) & 1 \end{bmatrix} = \mathbf{M}_2 \tag{7}$$

Then, the transformed functions to describe the wire trajectory of turning an angle θ are

$$\bar{y} = y + x\cot\theta = \delta \exp(-x/b) + x\cot\theta, \text{ for } \theta < \pi/2 \tag{8a}$$

$$\bar{y} = y + x\cos\theta = \delta \exp(-x/b) + x\cos\theta, \text{ for } \theta > \pi/2 \tag{8b}$$

Fig. 3(b) shows the fitted curves corresponding to the corners of $\theta = \pi/4$, $\pi/2$, and $3\pi/4$, respectively. For example, the fitted trajectory C_1 which corresponds to a turning angle of $\theta = \pi/4$, is obtained by transformation of the exponential function of a right-angle cutting with matrix $\mathbf{M}_1$. Curve C_2 represents that of $\theta = 3\pi/4$, and it is obtained by transformation with the use of matrix $\mathbf{M}_2$.

Eq. (3) can be employed to analyze MRR in the corner cutting process once the discharge-angle is obtained. As illustrated around point W of Fig. 4, the discharge-angle at an arbitrary point of the wire trajectory can be divided into two parts, $\hat{\theta}$ and ϕ, that is,

$$C_\theta = \hat{\theta} + \phi \tag{9}$$

where $\hat{\theta}$ is the angle spanned by a normal vector $\overrightarrow{WU}$ at point W of the wire trajectory and the unit vector of x-axis. It is evident from the triangular ΔWUV that $\hat{\theta} = \pi/2 - \theta_T$ where θ_T is the

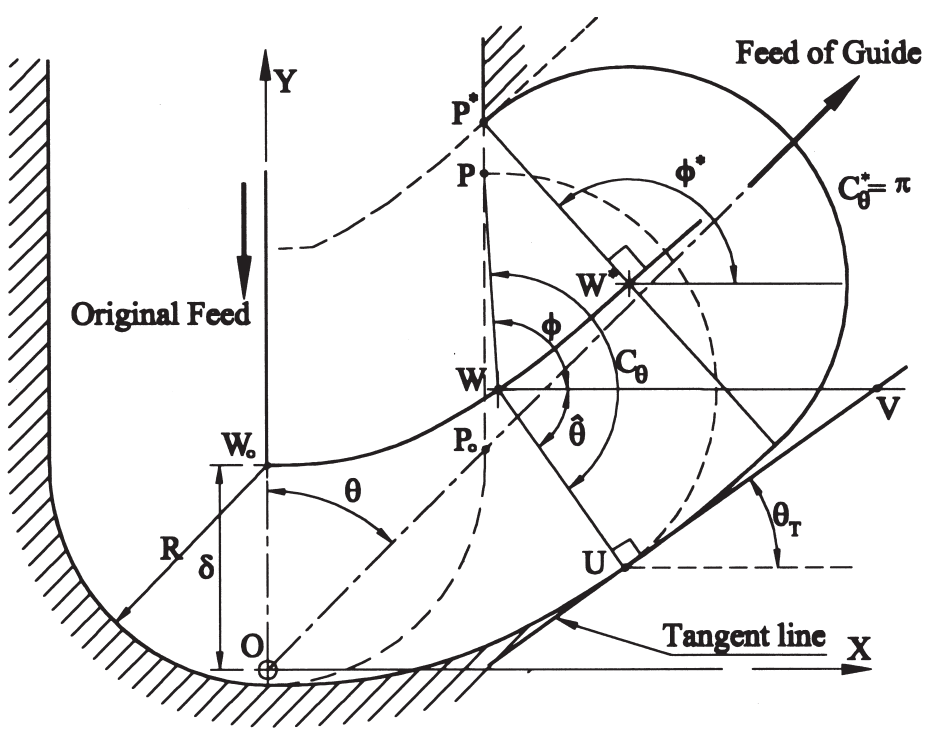

Fig. 4. Computational model of MRR in cutting a corner with an angle of θ.

tangent angle evaluated by the derivative of fitted function, i.e. $\tan\theta_T = d\bar{y}/dx$, at a specified point of the wire trajectory.

As depicted in Fig. 4, the intersection angle, ϕ, is defined as the angle spanned by the vector $\overrightarrow{WP}$ and the unit vector of x-axis, where point P is the intersection point of discharge-circle and the boundary of the kerf. The intersection angle can be obtained from the equation of boundary, $x = R$, and x component of the vector $\overrightarrow{OP}$. The position vector $\overrightarrow{OP}$ is the resultant of vectors $\overrightarrow{OW}$ and $\overrightarrow{WP}$. The x component of vector $\overrightarrow{OW}$ is obtained from the transformed curve and the vector $\overrightarrow{WP}$ is specified by a radial vector, $[R\cos\phi, R\sin\phi]$, of discharge-circle located at the wire centre.

Therefore, an equation $x + R\cos\phi = R$ is obtained for $\theta \leq \pi/2$ and the intersection angle ϕ can be written as:

$$\phi = \cos^{-1}(1 - \frac{x}{R}) \tag{10}$$

Otherwise, $x\sin\theta + R\cos\phi = R$ is resulted for $\theta > \pi/2$ and ϕ can be written as:

$$\phi = \cos^{-1}(1 - \frac{x\sin\theta}{R}) \tag{11}$$

As the wire centre moves from point W_o to point W*, the intersection point P moves from point P_o toward P* till vector $\overrightarrow{WP}$ coincides with the normal vector of the trajectory, which is $\overrightarrow{W^*P^*}$. Thereafter, the intersection angle is denoted as ϕ^*, where $\phi^* = \pi/2 + \theta_T$. From Eq. (9) and the fact of $\hat{\theta} = \pi/2 - \theta_T$, it is obvious that the discharge-angle C_θ is equal to π ever since.

Since the discharge-angle is obtained, the uncut thickness of workpiece and thus the MRR can be obtained by using Eqs. (1) and (2) in continuous time system, or Eq. (3) in discrete time system.

In the derivation of MRR in corner cutting, there are two advantages in fitting the wire trajectory to the transformed exponential function. Firstly, only two parameters, δ and b, are involved in the curve fitting. In fact, parameter δ is determined by the initial wire lag in straight-path cutting. Secondly, it is simple to determine the tangent angle at an arbitrary point of the trajectory because the fitted function is continuous with smooth derivative.

2.3. Guide's position relative to the wire centre

The above derivations are based on the assumption of given wire trajectory, in fact, the guide's position has not been specified yet. Since what we can obtain from the CNC unit in general WEDM process is the guide's position, in order to compare the theoretical MRR with experimental results, the guide's position relative to the given wire trajectory should be estimated. Because the relative displacement between wire electrode and guides is effected by discharging load, the direction of discharging load exerted on the wire surface is needed and it is derived and

given in the Appendix A. The direction of the resultant discharging load is described with a directional angle α with respect to the tangent line of wire trajectory.

Fig. 5 shows the geometrical relationship of the estimated guide's position with the given wire trajectory. As illustrated in Fig. 5, suppose that the main forces exerted on wire are the dragging force of guide, $\vec{g}$, and the discharging load, $\vec{e}$. The centripetal force, $\vec{n}$, which makes wire electrode move along the curved path, is determined by the resultant force of $\vec{g}$ and $\vec{e}$. Due to the fitted exponential function, the curvature of wire trajectory is very small at most points of the fitted trajectory, except the turning point W_o. Since the machine feedrate is assumed to be slow in the analysis, the centripetal force is very small at most points.

As depicted in Fig. 5 around point W, θ_G is defined as the directional angle of the vector $\overrightarrow{WG}$ in corner cutting, where point G denotes the guide's position. It is obvious that the directional angle of $\overrightarrow{WG}$ approaches θ_T as the wire trajectory approaches the guide's path. In straight-path cutting, the direction of dragging force is just in the opposite of the direction of discharge-load. The directional angle of $\overrightarrow{WG}$ is approximated to $\theta_T - \alpha$ as the wire turning a corner. Therefore, the directional angle, θ_G, ranges from $\theta_T - \alpha$ to θ_T according to the fitted trajectory. In order to simplify the calculation, the directional angle of guides is taken as the average of $\theta_T - \alpha$ and θ_T. In other word, θ_G is approximated by $\theta_T - \alpha/2$.

The guide's position, G, can be determined from the intersection of guide's path, $y = nx$, and the extension line from wire centre $W(\bar{x}, \bar{y})$ to the guide, i.e. $y - \bar{y} = m \cdot (x - \bar{x})$. The constant $n = \tan(\pi/2 - \theta)$ and the variable $m = \tan(\theta_T - \alpha/2)$ are their slopes. Hence, x coordinate of the intersection point is obtained as $x_G = (\bar{y} - m\bar{x})/(n - m)$, and the displacement of guides measured from the apex of a corner is $\overrightarrow{OG} = x_G \cdot csc\theta_G$.

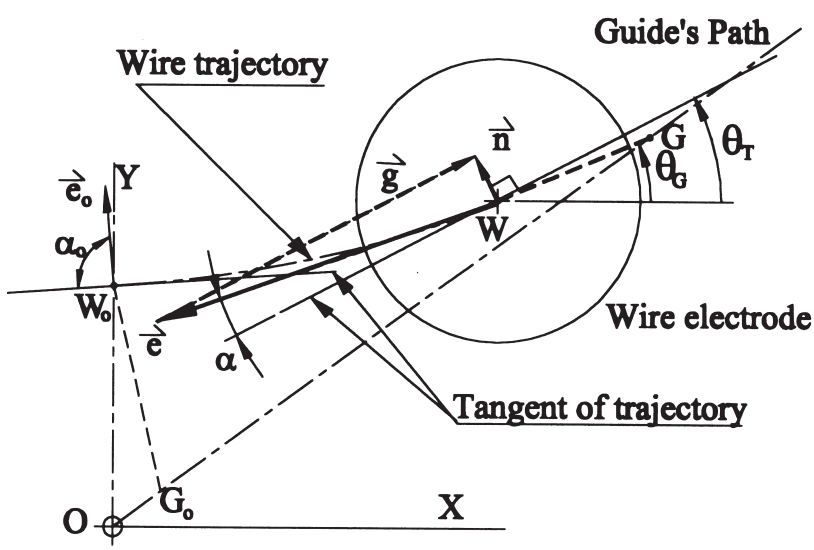

Fig. 5. Estimation of guide's position with respect to the given trajectory of wire centre and guide's path.

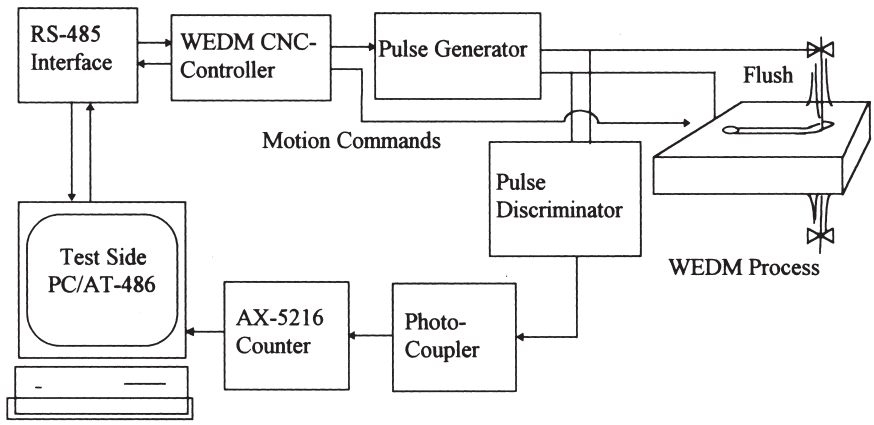

Fig. 6. Experimental set-up for WEDM frequency measurement.

3. Experimental result and discussion

Because it is difficult to measure the actual MRR in corner cutting, a series of sparking frequency experiments were performed to verify the proposed computational model of MRR. In these experiments, the amount removed by of each spark is assumed to be constant since the WEDM is an iso-energy type, and hence, the measured sparking frequency can be considered to be proportional to the actual MRR.

Fig. 6 shows the experimental set-up for sparking frequency measurement. The WEDM machine having an iso-energy pulse generator is controlled by a PC-based CNC controller developed by ITRI, Taiwan. Normal sparks and abnormal sparks were detected by a pulse discriminator attached to the pulse generator[7]. The number of EDM sparks in each sampling interval was counted by an AX-5216 counter through a photo-coupler. Table feed rate, tool position and discharging off-time were transmitted from the CNC controller to the test-side PC through a RS-485 interface. An PC/AT-486 personal computer was employed as the test-side node to collect the measured data. Since sparking frequency in the experiment may range up to 80 kHz and the machining feed rate is quite low, a sampling period of 100 ms was chosen.

Table 1 shows the WEDM operating conditions for the corner cutting experiments. In the experiments, a 0.25 mm diameter copper wire was used to cut a tool steel workpiece having a uniform 30 mm thickness. After several straight-path test cuts using the machining conditions of

Table 1
The operating conditions of WEDM experiment

Mechanical conditions	Machine feedrate	Wire tension	Wire feedrate	Upper flush pressure	Lower flush pressure
	2.15 mm/min	1200 gf	5 m/min	6.0 kg/cm^2	7.0 kg/cm^2
Electrical conditions	On-time	Off-time	Servo voltage	Open voltage	Machining voltage
	0.5 μs	16.0 μs	50 V	110 V	220 V

Table 1, the discharge-radius R and the wire lag δ determined from the cut kerf were 200 μm and 100 μm, respectively. Another curve fitting parameter was determined from the kerf of a right-angle cutting as $b = 600$ μm. Then the discharge-angle C_θ and the theoretical estimate of MRR was calculated by Eqs. (9) and (3), respectively.

Experiments were carried out for some typical geometrical cuttings as shown in Fig. 7(a). The points from A to E in the figure indicate corner angles of 150°, 120°, 90°, 60°, and 30°, respectively, and the solid line indicates machined path reported by the CNC unit. Fig. 7(b) shows the theoretical MRR (solid line) and the sparking frequency (dotted line) in corner cutting; both of them are functions of time. To compare the sparking frequency of WEDM and the theoretical MRR in the same scale, the relative percentage with respect to their level of straight-path cutting was employed.

As shown in Fig. 7(b), the computed MRR and the measured sparking frequency drop drastically as the wire electrode turns a corner. The amount of the drop at the corner apex depends on the angle of the corner being cut. The computed MRR agrees very well with the sparking frequency, except that the rise of sparking frequency after each valley lags behind that of theoretical

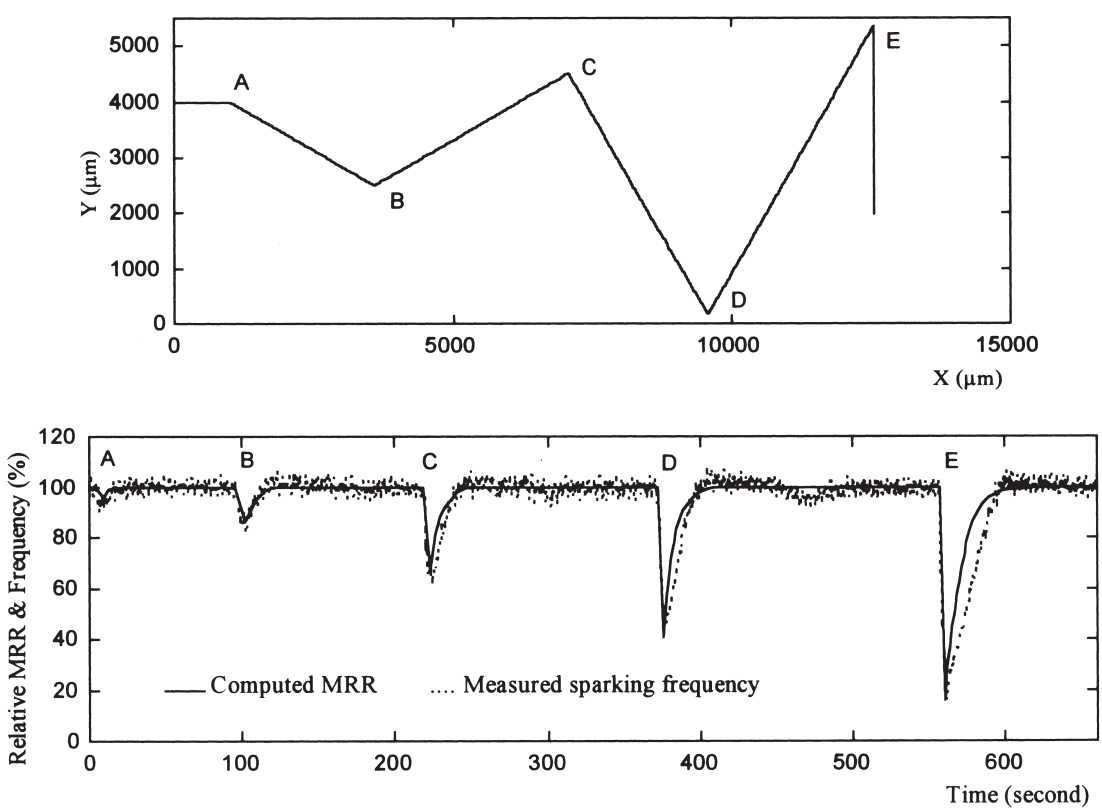

Fig. 7. (a) Recorded machining path of guides for corners of 150°, 120°, 90°, 60°, and 30° (from A to E); (b) computed MRR (solid line) and measured sparkling frequency (dotted line) with respect to the level of straight-path cutting (38 kHz).

MRR. This mismatch may be attributed to varying discharge-radius, which was not taken into account in the analysis.

In a report on finishing process by Magara et al. [14], the averaged gap-voltages, V_g, were proven to be linearly dependent on the sparking frequency, f_T. The relationship can be described with a simple equation $V_g = V_o - \kappa f_T$, where V_o is the open voltage and κ is a positive coefficient depending on the electrical conditions. Therefore, the abrupt increase of gap-voltage in corner cutting can also be interpreted as the result of the change of MRR.

Another singular phenomenon is the slight decrease of sparking frequency occurred between corners D and E. It is noted that the flush pressure reduced just after finishing a corner cutting. It is also observed that the sharper the turning corner is, the more severe the pressure drops after that corner. One of the causes can be attributed to the overlapped kerf around a corner, which induces more leakage of high pressure water. Due to the limitation of the instrumentation, it is conjectured that the decrease of sparking frequency between corners D and E is due to the variation of flush variations.

On the other hand, the CNC positioning error of table motion around corners is another factor to effect the sparking frequency. However, the positioning error, which is in the order of 1 μm can be considered as a minor factor in comparison with the deflection of wire, which is in the order of 100 μm.

The valley of sparking frequency at each apex and the recovering time of sparking frequency are compared with those of the theoretical MRR, and they are shown in Fig. 8. In the figure, the valley of sparking frequency and theoretical MRR is defined as the percentage of the minimum value at each corner apex with respect to the level of straight- path cutting. The recovering time of sparking frequency and the theoretical MRR is defined as the time interval from the beginning of corner cutting to the time when 95% of the level of straight-path cutting is recovered.

As seen from Fig. 8(a), the valleys of sparking frequency and MRR have the similar trend and they are related to the corner angle with a special relationship. It can be seen that the valleys approach 0% and 100% as the turning corner approaches 0° and 180° (straight-path cutting), respectively. The trend can be interpreted by an ideal model of MRR in which a rigid rod is used instead of the wire. As stated in Section 2.1, the discharge-angle, C_θ, at the instant of turning a corner for an ideal model is equal to the corner's angle, θ. Hence, assuming the constant feedrate and discharge-radius, the valley of ideal MRR is derived from Eqs. (1) and (2) as $(1 - \cos\theta)/(1 - \cos\pi)*100\%$, as shown by the dashed line in Fig. 8(a). The deviation of measured frequency from the ideal MRR is mainly caused by the wire deflection, and it is noted that the sharper corner induces the larger deviation.

Recovering times of actual sparking frequency and theoretical MRR in cutting various corners are presented in Fig. 8(b). It is evident from Fig. 8(b) that the recovering times of theoretical MRR and sparking frequency are almost inversely proportional to the corner angle. The recovering times of actual sparking frequency and theoretical MRR are very close. A longer recovering time is required in cutting a sharper corner since the kerf overlap in cutting a sharper corner is larger.

4. Conclusion

A useful concept of discharge-angle C_θ has been introduced and a systematic analysis for metal removal rate (MRR) in corner cutting has been presented. The MRR of general geometrical cutting

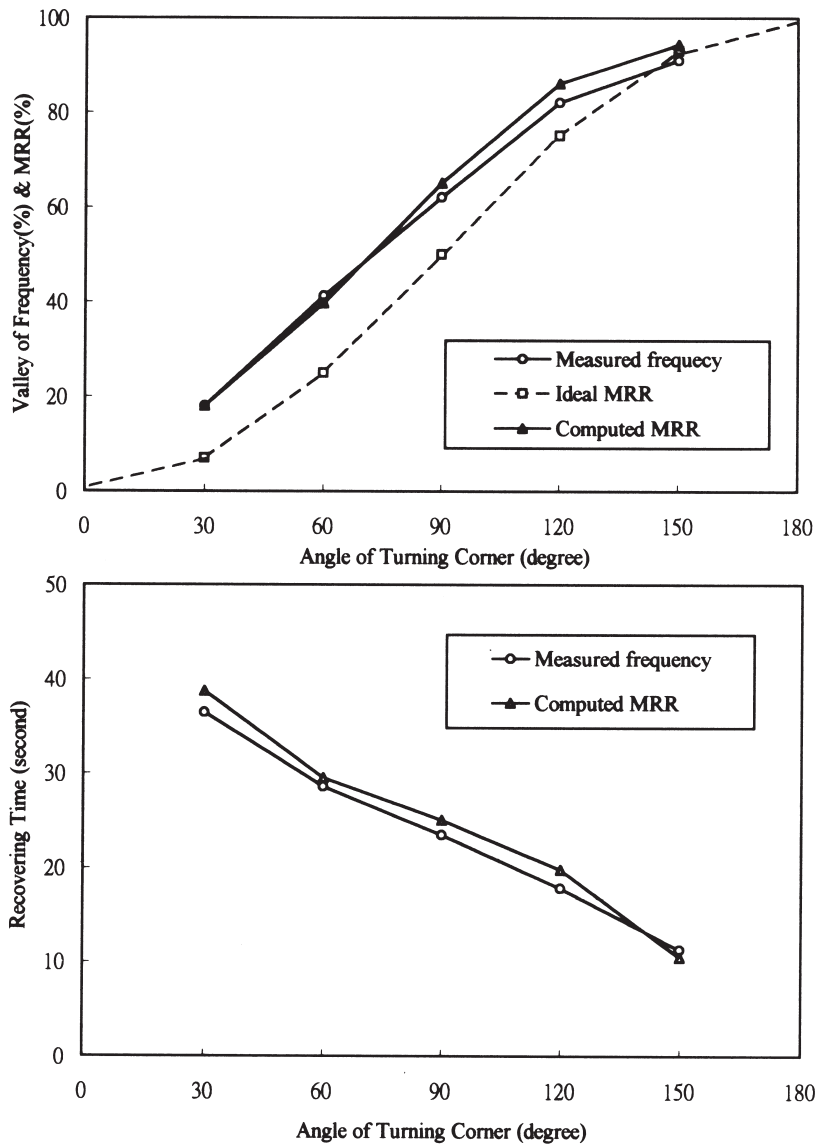

Fig. 8. Comparison of (a) valley and (b) recovering time of the measured sparking frequency and theoretical MRR.

has been estimated by a simple formula. Theoretical computation shows that both discharge-angle C_θ and MRR drop drastically to a minimum, then, they recover to the same level of straight-path cutting sluggishly. The amount of the drop at the corner apex is dependent on the angle of the turning corner.

The experimental results show that the theoretical MRR agrees very well with the variation of measured sparking frequency. The drastic variation of sparking frequency in corner cutting can be interpreted as the symptom of the abrupt change of MRR. The sudden increase of gap-voltage can also be interpreted as the result of abrupt MRR drop. Moreover, the varying MRR representing

the evolution of machining load of WEDM in corner cutting, which was considered as unknown disturbance in the past, can now be interpreted by geometrical analysis in this paper.

To extend the application of the present analysis, control of the sparking frequency and the strategies to improve the geometrical accuracy of WEDM process are underway.

Acknowledgements

Support from National Science Council, Taiwan, is gratefully acknowledged.

Appendix A: Derivation of the direction of resultant discharge-load

A computational model of discharge-load in straight-path cutting was proposed by Obara et al. [9]. Due to the asymmetric uncut workpiece with respect to the feed direction in corner cutting, the wire-electrode is subjected to different discharging load both in magnitude and direction as compared with straight-path cutting. By modifying Obara's model, the asymmetric load can be estimated by integrating the product of force components and probability distribution of sparks along the discharge-angle.

Fig. 9 presents the modified computational model of discharge-load. The geometrical relationship of an asymmetric uncut workpiece in cutting a corner is shown in the figure. Let f_T represent the sparking frequency, and let $f_r = f_T/H$ denote the uniform distribution of sparking frequency

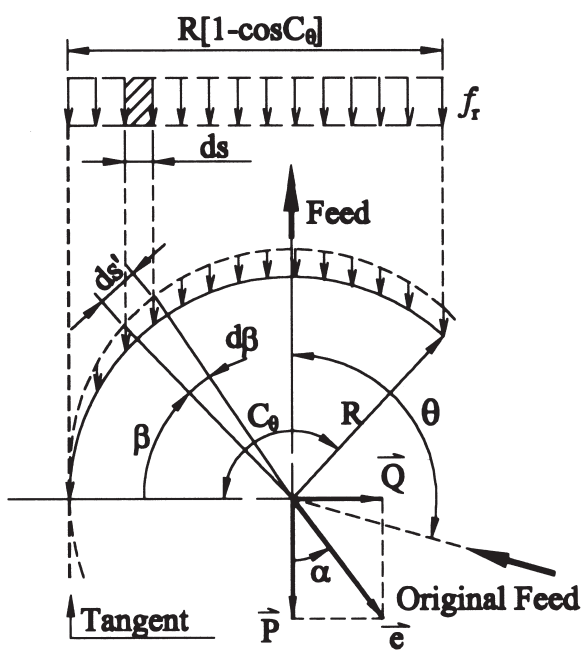

Fig. A1. Computational model of asymmetric discharging load in corner cutting.

per unit length of wire in the feed direction, then, as illustrated in Fig. 9, a small sector of wire electrode ds' at the angle, β, shares the following sparks distribution,

$$f_r \frac{ds}{R\cdot[1-\cos C_\theta]} = \frac{f_r \sin\beta\cdot d\beta}{1-\cos C_\theta} \tag{A1}$$

where $ds = ds'\sin\beta = R\sin\beta d\beta$.

As depicted in Fig. 9, the magnitude of the normal load P and that of the lateral load Q can be evaluated by the following equations:

$$P = \int_0^{C_\theta} \Delta F \sin\beta\cdot \frac{f_r \sin\beta}{1-\cos C_\theta}\,d\beta \tag{A2}$$

$$= \frac{\Delta F\cdot f_T}{(1-\cos C_\theta)H}\cdot\frac{2C_\theta - \sin 2C_\theta}{4}$$

$$Q = \int_0^{C_\theta} \Delta F \cos\beta\cdot \frac{f_r \sin\beta}{1-\cos C_\theta}\,d\beta \tag{A3}$$

$$= \frac{\Delta F\cdot f_T}{(1-\cos C_\theta)H}\cdot\frac{1-\cos 2C_\theta}{4}$$

where the single discharging impulse ΔF (in the unit Ns) can be obtained from the following equation [8]:

$$T\cdot\frac{d^2Y}{dz^2} - \frac{\pi}{4}\cdot f_T\cdot\Delta F = 0 \tag{A4}$$

where direction of Y, Z coordinates and the tension, T, are shown in the configuration of WEDM process of Fig. 1(a). The directional-angle, α, of the resultant load measured from the opposite of feed direction can be written as follows:

$$\alpha = \tan^{-1}\left(\frac{Q}{p}\right) \tan^{-1}\left(\frac{1-\cos 2C_\theta}{2C_\theta - \sin 2C_\theta}\right) \tag{A5}$$

References

[1] W.L. Dekeyser, R. Snoeys, Geometrical accuracy of wire-EDM, 9th Int. Symp. on ElectroMachining (ISEM-9), Japan, 1989, pp. 226–232.

[2] K.P. Rajurkar, W.M. Wang, WEDM identification and adaptive control for variable height components, Annals of CIRP 43 (1) (1994) 199–202.

[3] N. Kinoshita, M. Fukui, G. Gamo, Control of wire-EDM preventing electrode from breaking, Annals of CIRP 31 (1) (1982) 111–114.

[4] K.P. Rajurkar, W.M. Wang, On line monitor and control for wire breaking in WEDM, Annals of CIRP 40 (1) (1991) 219–222.
[5] K. Shoda, Y. Kaneko, H. Nishimura, M. Kunieda, M.X. Fan, Adaptive control of WEDM with on-line detection of sparc locations, 10th Int. Symp. on ElectroMachining (ISEM-10), Germany, 1992, pp. 410–416.
[6] M.T. Yan, Y.S. Liao, Monitoring and self-learning fuzzy control for wire rupture prevention in wire electrical discharge machining, International Journal of Machine Tools & Manufacture 36 (3) (1996) 339–353.
[7] M.T. Yan, Y.S. Liao, Adaptive control of WEDM process using fuzzy control strategy, 11th Int. Symp. on Electro-Machining (ISEM-11), Switzerland, 1995, pp. 343–352.
[8] H. Obara, Y. Makino, T. Ohsumi, Single discharging force and single discharging volume of wire EDM, 11th Int. Symp. on ElectroMachining (ISEM-11), Switzerland, 1995, pp. 85–93.
[9] N. Kinoshita, M. Fukui, Y. Kimura, Study on the wire EDM: in process measurement of mechanical behavior of electrode wire, Annals of CIRP 33 (1) (1984) 89–92.
[10] H. Sthioul, R. Delpretti, C. Tricarico, D.F. Dauw, Improvement of the wire EDM cutting precision by vibration analysis and control, 9th Int. Symp. on ElectroMachining (ISEM-9), Japan, 1989, pp. 214–218.
[11] D.F. Dauw, High precision Wire-EDM by on-line wire position control, Annals of CIRP 43 (1) (1994) 193–197.
[12] Z. Jian, C.Y. Yu, A new control strategy for sharp corner cutting in wire EDM, 10th Int. Symp. on ElectroMachining (ISEM-10), Germany, 1992, pp. 353–358.
[13] T. Magara, T. Yatomi, H. Yamada, K. Kobaynshi, Study on machining accuracy in WEDM, part I—improvement of machining accuracy of corner parts in rough-cutting (in Japanese), Journal of Japan Society of Electrical-Machining Engineers 25 (49) (1991) 23–32.
[14] T. Magara, T. Yatomi, H. Yamada, K. Kobaynshi, Study on machining accuracy in WEDM, part II—improvement of machining accuracy of corner parts in rough-cutting (in Japanese), Journal of Japan Society of Electrical-Machining Engineers 26 (52) (1992) 1–15.